

# Pion-Pion Elastic Scattering, Dynamical Generation of the $f_0(500)$ Resonance, Finite-temperature effects and Chiral Restoration: A Large-N Approach

Santiago C<sup>1\*</sup>, Nicola AG<sup>2</sup>, John Morales<sup>3</sup> and Jose RR<sup>1</sup>

<sup>1</sup>Departamento de Física, Univ. de Los Andes, 111711 Bogota, Colombia

<sup>2</sup>Departamento de Física Teórica II. Univ. Complutense. 28040 Madrid. Spain

<sup>3</sup>Departamento de Física, Univ. Nacional de Colombia, 111321 Bogota, Colombia

## Short Communication

Received date: 08/02/2017

Accepted date: 17/02/2017

Published date: 24/02/2017

### \*For Correspondence

Santiago C, Department de Física, University of Los Andes, Bogotá, Colombia,  
Tel: +57 1 3394949.

**E-mail:** js.cortes125@uniandes.edu.co

**Keywords:** Chiral lagrangians, Finite-temperature field theory, Large N expansions, Chiral symmetries

### ABSTRACT

In this work, we discuss and summarize three large N approaches given to analyze how a set of massless pions behave at finite temperature. The first one focuses in the problem of obtaining thermal phase shifts, where the others aim to study chiral symmetry restoration phenomena. All the results are achieved by considering an  $O(N + 1)/O(N)$  nonlinear sigma model where N is the number of pions (or Nambu-Goldstone bosons) involved, in which thermal effects are introduced via the imaginary time formalism.

## INTRODUCTION

Low-energy critical phenomena such as chiral symmetry restoration are needed for a better understanding of the behavior of hadronic matter created in relativistic heavy ions collisions (e.g. LHC-ALICE). A very adequate approach with outstanding results is given by lattice simulations <sup>[1-4]</sup>, where physical observables such as chiral critical temperatures and exponents are obtained. Some theoretical advances can be made if and only if they fulfill the conditions given in the low energy regime of QCD, as showed by Chiral Perturbation Theory (ChPT) momentum expansions extended to the finite-temperature regime involving light mesons <sup>[5,6]</sup>, or Nambu - Jona-Laisino (NJL)-like models <sup>[7]</sup>, in which quark fields are taken as the degrees of freedom. These models include an explicit chiral symmetry breaking term that induces mass to the fields involved.

Here we consider a nonlinear sigma model of N self-interacting massless pions and a field in which a scalar resonance (the  $f_0(500)$ ) is dynamically generated, thus breaking the chiral symmetry <sup>[8,9]</sup>. The  $f_0(500)$  has the same quantum numbers as a QCD vacuum state, and is susceptible to chiral symmetry restoration effects. In order to attain this, temperature is introduced via self-energy and scattering loop corrections <sup>[10,11]</sup>, and three approaches are considered in order to study two sort of phenomena: thermal effects on scattering phase shifts <sup>[12]</sup> and chiral symmetry restoration through scattering <sup>[13,14]</sup> and generating functional developments <sup>[15]</sup>; in these two last works, we obtain a second-order phase transition after considering a regime where the temperature is below its chiral critical value  $T \approx 150 - 160$  MeV.

## LARGE N EXPANSION FOR LEQCD IN THE CHIRAL LIMIT

We begin by considering a  $O(N + 1)/O(N)$  nonlinear sigma model for massless pions whose Lagrangian reads <sup>[8,9]</sup>

$$\mathcal{L} = \frac{1}{2} g_{ab}(\pi) \partial_\mu \pi^a \partial^\mu \pi^b, \quad (1)$$

Where the vacuum constraint and metric induced by it read, respectively,

$$f_\pi^2 = NF^2 \quad (2)$$

$$g_{ab}(\pi) = \delta_{ab} + \frac{\pi_a \pi_b}{NF^2 \left(1 - \frac{\pi_a^2}{NF^2}\right)} \tag{3}$$

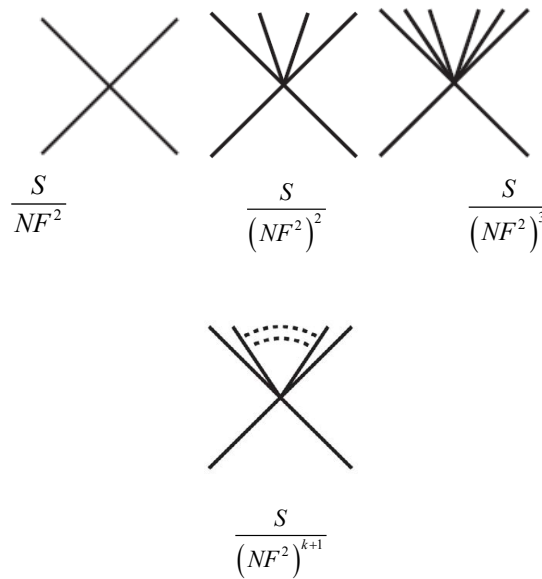


Figure 1. Tree-level Feynman diagrams and rules for pion-pion scattering.

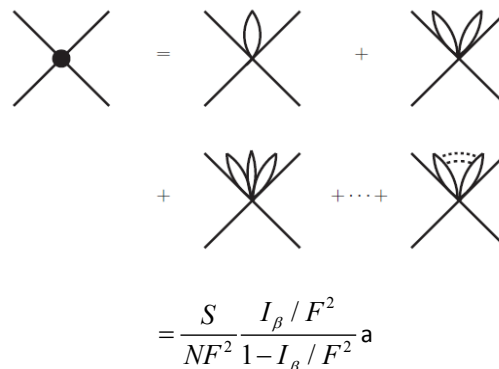


Figure 2. The scattering Feynman rules and diagrams.

The scattering Feynman rules and diagrams are obtained after expanding the non-diagonal term in (3), thus yielding the results shown in **Figure 1**.

All the scattering rules are written in terms of the Mandelstam variables.

We can consider among three approaches to analyze Finite-Temperature pion phenomena in the chiral limit:

1. Isolating the 4-pion vertex and separating the dynamics at zero and finite temperature so thermal phase shifts can be studied.
2. Building up an effective interaction vertex with all the tree-level diagrams and dynamically generate a scalar resonance ( $\sigma/f_0(500)$ ); since this resonance is associated to chiral symmetry breaking, thermal effects will allow us to check whether this symmetry is to be (or not to be) restored.
3. Introducing an explicit symmetry breaking term in such a way that a very small pion mass is generated. As in the previous item, we will study restoration of broken symmetries, although using a diagrammatic analysis for partition functions.

**1<sup>ST</sup> Approach: Dynamics of Massless Pions at Finite Temperature**

We build up an effective Thermal Vertex (ETV) as it is shown in **Figure 2**: here we close every pair of extra pion lines that come from the  $1/N$  expansion of the nonlinear metric (3) in such a way that only four external legs are involved. All the closed ring diagrams correspond to tadpoles whose contribution is  $N I_\beta$ . This allows us to take into account any effect associated to the presence of a thermal bath in the scattering dynamics, something that we schematically exhibit in the diagrams of **Figure 3**, where we label the scattering amplitudes as  $[l;m]$ ; in this case,  $l$  is the number of ETV's considered and  $m$  indicates if there is any initial scattering loop (as it is shown in the diagram for  $[2; 1]$ ).

Since pions are massless, we do not have to deal either with mass or wave function renormalization<sup>1</sup>; instead of these, the divergence comes from the scattering loop integral  $I_\beta(S)$ , whose explicit dimensionally regularized form reads

$$I_\beta(S) = -\frac{N_\epsilon}{16\pi^2} - \frac{1}{16\pi^2} \ln\left(\frac{-s}{\mu^2}\right) + \bar{I}(s, \beta), \tag{4}$$

and where the thermal (and finite) contribution is given by

$$\bar{I}(s, \beta) = \frac{1}{2\pi^2} \left[ \bar{I}_M(s, T) + \bar{I}(s, T)_0 \right], \tag{5}$$

$$\bar{I}_M(s, T) = \sum_{j=0}^{\infty} \left\{ \frac{1}{(2j-1)^2} - \frac{1}{4j(j-1)} + \sum_{m=1}^{\infty} \frac{B_{2m}}{[2(j+m)-1](2m)!} \right\} \left( \frac{2T}{\sqrt{s}} \right)^{2j}, \tag{6}$$

$$\bar{I}_M(s, T)_0 = \frac{T}{4\sqrt{s}} \left[ Li_2\left(\frac{T^2}{s}\right) - 4Li_2\left(\frac{T}{\sqrt{s}}\right) \right]. \tag{7}$$

In this case, is the renormalization scale of the loop integral (4), whilst  $B_{2m}$  are Bernoulli numbers and  $Li(x)$  is the logarithm integral function? We obtained the latter finite-temperature results by considering that the energy of the pions of the loops  $E$  is such that  $E < \sqrt{s}$  and  $E < T$ , where  $T$  is the temperature of the thermal bath<sup>[12-17]</sup>. The renormalization is attained after redefining both the four-pion and the  $ETV$  as follows:

$$\frac{s}{NF^2} \frac{I_\beta / F^2}{1 - I_\beta / F^2} \rightarrow \frac{s}{NF^2} \frac{I_\beta / F^2}{1 - I_\beta / F^2} H_0(s). \tag{8}$$

$$\frac{s}{NF^2} \frac{I_\beta / F^2}{1 - I_\beta / F^2} \rightarrow \frac{s}{NF^2} \frac{I_\beta / F^2}{1 - I_\beta / F^2} H_0(s). \tag{9}$$

$G_0(s)$  and  $H_0(s)$  are bare couplings whose function is to absorb the pole given in (4), as shown below:

$$\begin{aligned} \frac{1}{G_R(s)} &= \frac{1}{G_0(s)} - \frac{sN_\epsilon}{32\pi^2}, \\ H_R^{(1)}(s) &= \frac{H_0(s)}{G_0^2(s)}, \\ H_R^{(2)}(s) &= N_\epsilon \frac{H_0(s)}{G_0(s)}, \\ H_R^{(3)}(s) &= \frac{H_0(s)}{G_0(s)}, \end{aligned} \tag{10}$$

Where  $N_\epsilon$  is a divergent quantity defined in the renormalization MS scheme. Thanks to this, we can write a finite (renormalized) amplitude  $A_R(s, \beta)$  such that

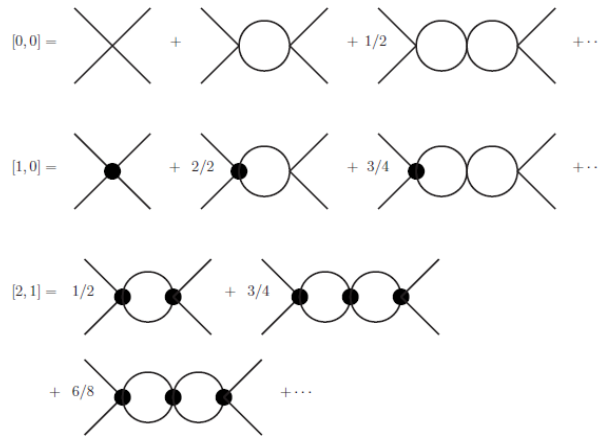


Figure 3. Zero and finite-temperature four-pion scattering amplitudes.

$$A_R(s, \beta) = \frac{s}{NF^2} \left\{ \frac{G_R(s)}{1 - \frac{sG_R(s)}{32\pi^2 F^2} \left[ \ln\left(\frac{-s}{\mu^2}\right) - 16\pi^2 \bar{T}(s, \beta) \right]} + \sum_{V=1}^M H_R^{(V)}(s) \left( \frac{I_\beta / F^2}{1 - I_\beta / F^2} \right)^V B_R(s, T, V) \right\}, \quad (11)$$

$$B_R(s, T, V) = \left( \frac{s}{32\pi^2 F^2} \left\{ H_R^{(2)}(s) + H_R^{(3)}(s) \left[ \ln\left(\frac{-s}{\mu^2}\right) - 16\pi^2 \bar{T}(s, \beta) \right] \right\} \right)^{V-1} \times \frac{1}{\left\{ 1 - \frac{sG_R(s)}{32\pi^2 F^2} \left[ \ln\left(\frac{-s}{\mu^2}\right) - 16\pi^2 \bar{T}(s, \beta) \right] \right\}^{V+1}} \quad (12)$$

After expanding the scalar channel  $l=j=0$  amplitude  $T_{l=j=0}(s, \cos \theta, \theta) = N A_R(s, \theta) + A_R(t, \theta) + A_R(u, \theta) \approx N A_R(s, \theta)^3$  in partial waves (considering the lowest order approximation:  $G_R(s) = H_R^{(1)}(s) = H_R^{(2)}(s) = H_R^{(3)}(s) = 1$ )

$$a_{00}(s) = \frac{1}{64\pi} \int_{-1}^1 N A_R(s) P_0(\cos \theta) d(\cos \theta) \quad (13)$$

We obtain the thermal phase shifts showed in **Figure 4**. As it can be seen, they monotonically increase as both the COM energy  $\sqrt{s}$  and the temperature  $T$  are enlarged [18-24].

Unfortunately, this approach has the following issues:

The renormalization procedure has a problem with the definition of  $H_R^{(2)}(s)$  and  $H_R^{(3)}(s)$  because  $H_R^{(3)}(s)/H_R^{(2)}(s) \rightarrow \infty$ . In order to renormalize properly these quantities, another bare coupling constant has to be added to the equation set 10, as shown for the massive case in ref. [8].

The finite-temperature integral  $\bar{T}(s, \beta)$  violates unitarity. The nonlinear sigma model is already unitarized in the energy range  $300 \text{ MeV} \leq \sqrt{s} \leq 700 \text{ MeV}$  since the scalar resonance  $\sigma/f_0(500)$  is considered in the dynamics.

Both  $F$  and  $\mu$  are not appropriate values to this chiral model. The values we consider are given for a massive nonlinear sigma model. In that case,  $(F, \mu) = (55; 775) \text{ MeV}$  [8].

All these problems are properly fixed in the next section.

$\sqrt{s}(\text{MeV})$

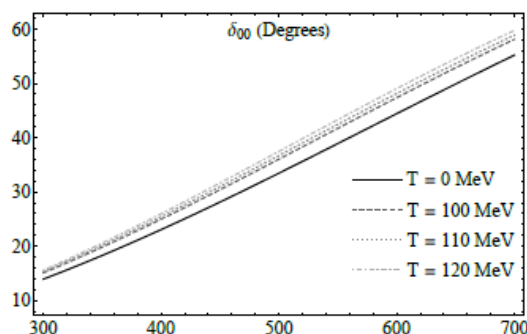


Figure 4. Phase shifts in the scalar channel considering three different values of temperature.

2<sup>nd</sup> Approach: The  $f_0(500)$  and Chiral Restoration

We define a new ETV by including the four pion term of **Figure 1** (the one without extra lines); this corresponds now to replace the function in **Figure 2** by

$$f(I_\beta) = \frac{s}{NF^2} \frac{1}{1 - I_\beta / F^2} \tag{14}$$

In this case, we separate the dynamics at zero and finite temperature by building two amplitudes: the first one where thermal bath effects are not considered, and the second one which introduces temperature thanks to (14) and to the thermal loops  $J(p;T)$  in it, as shown in **Figure 5**. In this case,  $J(p;T)^4$  reads

$$J(p;T) = J_\epsilon(\mu) + J_{fin}(p;T;\mu), \tag{15}$$

Where  $J_{fin}(p;T;\mu)$  also includes the zero-temperature finite term given by

$$\frac{1}{16\pi^2} \ln\left(\frac{\mu^2}{-s}\right), \tag{16}$$

and the divergent term is given in dimensional regularization as <sup>[18]</sup>

$$J_\epsilon(\mu) = \frac{1}{16\pi^2} \left[ \frac{2}{\epsilon} + \ln 4\pi - \gamma + 2 - \ln \mu^2 \right] + \mathcal{O}(\epsilon). \tag{17}$$

The renormalization of the amplitudes  $A(s)$  and  $A(p;T)$  in **Figure 5** is adequately attained after redefining the vertices as  $\frac{s}{(NF^2)^{k+1}} \rightarrow \frac{s}{(NF^2)^{k+1}} G_0^{k+1}(s), k=0,1,2,3,\dots$ , thus yielding a finite coupling  $G_R(s,\mu)$  such that:

$$\frac{1}{G_R(s,\mu)} = \frac{1}{G_0(s)} - \frac{sJ_\epsilon(\mu)}{2F^2}. \tag{18}$$

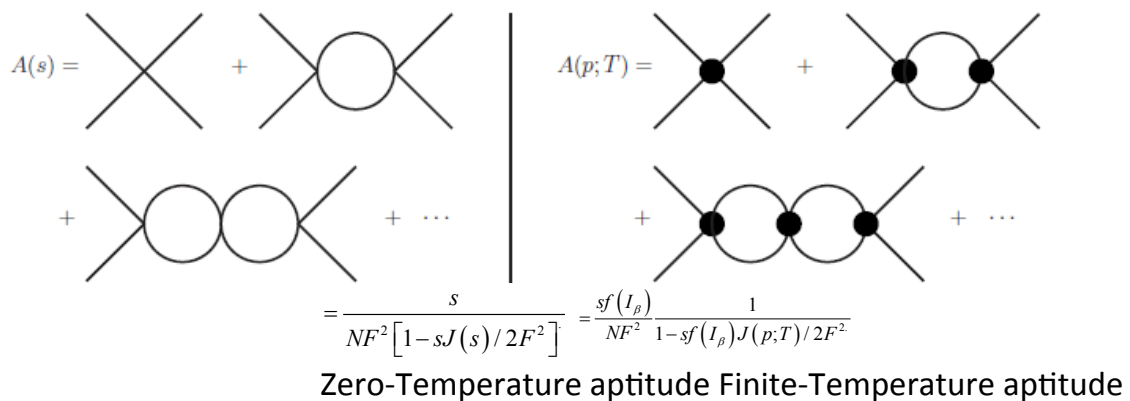


Figure 5. Zero and Finite-Temperature amplitudes in the s channel.

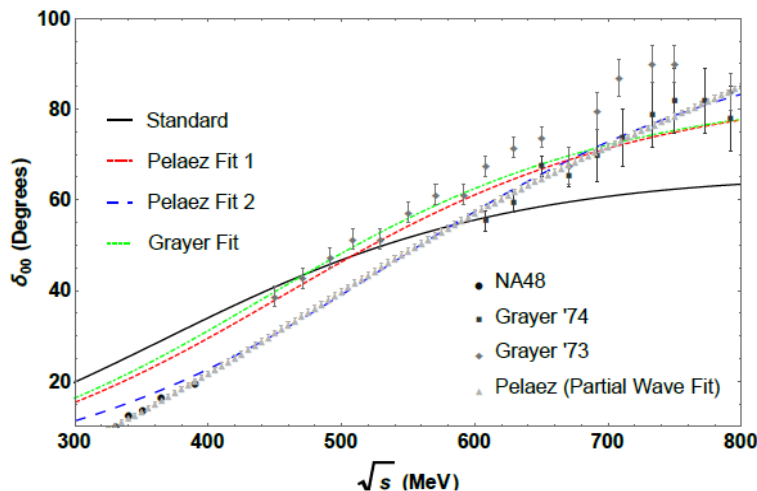


Figure 6. Scalar susceptibility as a function of T for the fits considered so far.

**Table 1.** Resonance positions in the complex plane and critical temperatures and exponents for the scalar susceptibility  $\chi_S(T)$ .

| Fit      | $T_c$ (MeV) | $M_p(0)$ (MeV) | $\Gamma_p(0)$ (MeV) | $\gamma_\chi$ | $R_{\gamma_\chi}^2$ |
|----------|-------------|----------------|---------------------|---------------|---------------------|
| Grayer   | 92.33       | 438.81         | 536.47              | 0.875         | 0.99987             |
| Peláez 1 | 96.00       | 452.42         | 546.26              | 0.938         | 0.99997             |
| Peláez 2 | 129.07      | 535.53         | 534.59              | 0.919         | 0.99995             |
| IAM      | 118.23      | 406.20         | 522.70              | 1.012         | 1                   |
| Standard | 61.20       | 356.97         | 566.05              | 0.842         | 0.99728             |

Since the partial wave decomposition 13 is also valid at nite temperature, we can check that this model holds exactly with unitarity in this regime (a fact that was imposed in the usual momentum expansion <sup>[24]</sup>). This allows us to check if the chiral symmetry is restored at a given value of temperature, something easily achieved after finding the resonance/pole in the second Riemann sheet by extending the energy to the complex plane as  $\sqrt{s}(T) = M_p(T) - i\Gamma_p(T)/2$ , and by defining a proper quantity such as the scalar susceptibility, whose behavior in the  $p=0$  limit is  $\chi_S(T) \propto 1 / \text{Re}\{s(T)\} = 1 / M_S^2(T)$  and its unitarized form reads <sup>[16]</sup>

$$\frac{\chi_S^U(T)}{\chi_S^{ChPT}(0)} = \frac{M_S^2(0)}{M_S^2(T)} \tag{19}$$

The behavior of (21) (taking into account our ts for the parameters, along with the IAM result in the chiral limit <sup>[16]</sup>) is shown in **Figure 6**, and our results concerning resonance position in the complex plane (mass and width), critical temperatures and critical exponents for  $\chi_S(T)$  are given in **Table 1** <sup>[13,14]</sup>.

Due to the lack of experimental data, we compare our  $T_c$  and  $\gamma_\chi$  values with the lattice values  $T_\chi = 154 \pm 9$  MeV <sup>[2]</sup> and  $\gamma_\chi = 0.54$  (three-dimensional O(4) model) <sup>[3]</sup>, along with the theoretical four-dimensional O(N) model  $\gamma_\chi = 1$  <sup>[25]</sup>. In this case, T is expected to decrease about 20% of its value. As it can be seen, our results agree with these bounds. In the other hand, our resonance parameters  $M_p(0)$  and  $\Gamma_p(0)$  are in good accordance with the most recent experimental bounds <sup>[26]</sup> and with the theoretical fit <sup>[23]</sup>, where  $M_p(0) = 457_{-13}^{+14}$  MeV and  $\Gamma_p(0) = 558_{-14}^{+22}$  MeV.

The reach of this works ends here, because order parameters as the scalar quark condensate (whose derivative in terms of the mass yields the scalar susceptibility  $\chi_S(T)$ ) cannot be found by taking the strict chiral limit. This is the aim of the next section.

**3<sup>rd</sup>. Approach: Large-N Partition Function for Massless Pions**

All we have to do so mass is to be considered is adding a massive term to the Lagrangian (1) (as shown in ref. <sup>[8]</sup>), i.e.,

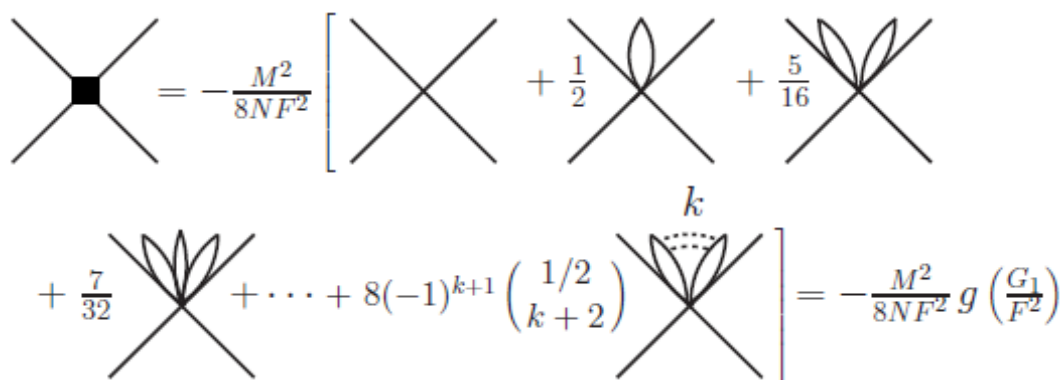


**Figure 7:** Effective mass vertex and its respective Feynman rule in the chiral limit.  $G_1(x)$  is taken as in ref. <sup>[5]</sup>.

$$\mathcal{L}_{NL\text{SM}} = \frac{1}{2} \left[ \delta_{ab} + \frac{1}{NF^2} \frac{\pi_a \pi_b}{1 - \pi^2 / NF^2} \right] \partial_\mu \pi^a \partial^\mu \pi^b + NF^2 M^2 \sqrt{1 - \frac{\pi^2}{NF^2}}. \tag{20}$$

After expanding the square root term in (22), we build an effective mass vertex as that given in **Figure 7**. Then, we construct the partition function as shown in **Figure 8**, where only the contributions given up to order  $\mathcal{O}(M^3 T)$  are to be taken into account when considering the limits  $M/F, M/T \rightarrow 0$  (any higher contribution induces mass divergences, something we want to avoid since their large N resummation becomes harder). Its explicit dependence on M, T and N is such that:

$$z(M, T) = -N \frac{\pi^2 T^4}{90} - NM^2 F^2 \left\{ 1 - \frac{T^2}{24F^2} + h\left(\frac{T^2}{12F^2}\right) \right\} - \frac{NM^3 T}{8\pi} \left\{ \frac{2}{3} - 2h\left(\frac{T^2}{12F^2}\right) + H\left[-\frac{1}{2}\tilde{g}\left(\frac{T^2}{12F^2}\right)\right] \right\} + \mathcal{O}[M^4 \log M, N^0], \tag{21}$$

Where the finite functions  $g(x)$ ,  $h(x)$  and  $H(x)$  are given by:

$$g(x) = -\frac{8}{x^2} \left[ \sqrt{1-x} - 1 + \frac{x}{2} \right], \tag{22}$$

$$h(x) = \sqrt{1-x} - 1 + \frac{x}{2}, \tilde{g}(x) = \frac{1}{\sqrt{1-x}} - 1, \tag{23}$$

$$H(x) = x^2 + 2 \sum_{n=3}^{\infty} \frac{(2n-5)!!}{n!} x^n = -\frac{2}{3} (1 - 3x - \sqrt{1-2x} + 2x\sqrt{1-2x}).$$

Since we are keeping a finite mass-dependent partition function, we can derive it in order to obtain the scalar quark condensate and take the chiral limit to check if there is an associated critical temperature, as it was made for the scalar susceptibility in section IV. The result normalized to  $\langle \bar{q}q \rangle(M, 0) = -2NF^2$  explicitly reads

$$\frac{\langle \bar{q}q \rangle(M, T)}{\langle \bar{q}q \rangle(M, 0)} = \sqrt{1 - \frac{T^2}{T_c^2}} + \mathcal{O}(M, N^0). \tag{24}$$

We plot the normalized condensate (26) as a function of T in **Figure 9**<sup>[15]</sup>, along with the results for the ChPT momentum expansion to different perturbative orders<sup>[5]</sup>. Here we obtain exact critical exponent  $\beta=0.5$  (and a critical temperature  $T_c = \sqrt{12}F \approx 174MeV$  - when taking the standard values for (F,μ)-, something that cannot be found in ChPT since the scalar condensate is a polynomial in the temperature.

### CONCLUSIONS

We have reviewed some recent approaches to chiral symmetry restoration within the large-N effective theory approach for the pion gas. Our first approach yields some inconsistencies related with unitarity and renormalization

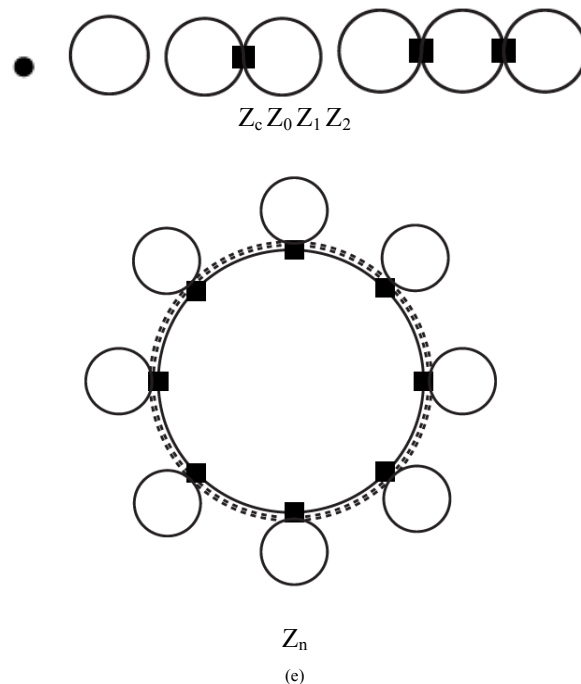


**Figure 8:** Relevant Feynman diagrams that contribute to the partition function to order  $\mathcal{O}(M^3 T)$ .

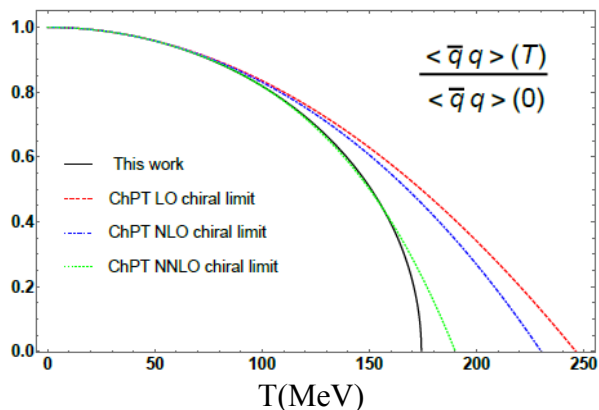


**Figure 9:** Normalized scalar quark condensate as a function of temperature for two different approaches.

Properties of the nonlinear sigma model; this made us reconsider how to build quantities as scattering amplitudes in such a way that those issues are to be avoided.

In our second approach, the analysis of elastic pion scattering at finite temperature in the large  $N$  expansion grants a description of the  $f_0(500)$  resonance dependence on  $T$  that is consistent with previous works [16]. Furthermore, there are two aspects to point out:

1. The behavior of  $\chi_S^{-1}(T)$  when considering saturation by the  $f_0(500)$  pole, is consistent with a second-order phase transition, as seen in the lattice [2].

2. Our  $T_c$  results are not far from the expected lattice values (as explained in section IV), and besides, they are even closer to the result obtained for NJL-like models ( $T_c \approx 100.7$  MeV.) [26].

We show in our third approach that scalar quark condensates can be obtained through a large  $N$  partition function, which is indeed finite since the mass divergences do not appear in the limits  $M/F$ ,  $M/T \rightarrow 0$ . Furthermore, our critical exponent  $\beta$  is found in an exact way, and coincides with the expected value for an  $O(N)$ -symmetric 4-dimensional Heisenberg model (a fact also checked in section IV) [25]. Nevertheless, the critical temperature is quite higher than in the scattering analysis; this is due to not considering the saturation of the  $f_0(500)$  resonance.

We expect to use another approaches, e.g., the virial expansion (S. Cortés, A. Gómez Nicola and J. Morales -in preparation-) and holographic models (S. Cortés, M. A. Martín Contreras and J. R. Roldán -in preparation-), so a broader map can be built to compare these sort of critical phenomena.

## ACKNOWLEDGMENTS

S.C. and J.R.R. thank Departamento de Física - Uniandes and Facultad de Ciencias - Uniandes for financial support. A.G.N. acknowledges financial support from the spanish research contracts FPA2014-53375-C2-2-P and FIS2014-57026-REDT.

## REFERENCES

1. Aoki Y, et al. The QCD transition temperature: results with physical masses in the continuum limit II. JHEP. 2009.
2. Bazavov A, et al. The chiral and deconfinement aspects of the QCD transition. Phys. Rev. D. 2012;85:054503.
3. Ejiri S, et al. On the magnetic equation of state in (2+1)- flavor QCD. Phys. Rev. D. 2009;80:094505.
4. Bhattacharya T, et al. QCD Phase Transition with Chiral Quarks and Physical Quark Masses. Phys. Rev. Lett. 2014;113.
5. Gerber P and Leutwyler H. Hadrons Below the Chiral Phase Transition. Nucl. Phys. B. 1989;321:387-429.
6. Gasser J and Leutwyler H. Light Quarks at Low Temperatures. Phys. Lett. B. 1987;184:83-88.
7. Bernard V, et al. Decoupling of the Pion at Finite Temperature and Density. Phys. Rev. D. 1987;36:819-836.
8. Dobado A and Morales J. Pion mass effects in the large  $N$  limit of  $\chi$ (PT). Phys. Rev. D. 1995;52:2878-2890.
9. Dobado A, et al. Effective lagrangians for the standard model. Springer-Verlag (Texts and Monographs in Physics), New York. 1997.
10. Kapusta JI and Gale C. Finite-temperature field theory: Principles and applications. 2006.
11. Le Bellac M. Thermal Field Theory. 1996.

12. Cortes S, et al. Dynamics of Massless Pions at Finite Temperature. Proceedings of the X Latin American Symposium of High Energy Physics. 2015.
13. Cortes S, et al. Large-N pion scattering at finite temperature: the  $f_0(500)$  and chiral restoration. Phys. Rev. D. 2016;93:036001.
14. Cortes S, et al. Large-N Pion Scattering, Finite-Temperature Effects and the Relationship of the  $f_0(500)$  with Chiral Symmetry Restoration. 2016.
15. Cortes S, et al. Chiral Symmetry Restoration for the large-N pion gas. Phys. Rev. D. 2016;94:116008.
16. Gomez Nicola A, et al. Chiral Symmetry Restoration and Scalar-Pseudoscalar partners in QCD. Phys. Rev. D. 2013;88:076007.
17. Weldon HA. Effective Fermion Masses of Order  $gT$  in High Temperature Gauge Theories with Exact Chiral Invariance. Phys. Rev. D. 1982;26:2789-2810.
18. Gasser J and Leutwyler H. Chiral Perturbation Theory to One Loop. Annals Phys. 1984;158:142-233.
19. Dobado A and Pelaez JR. On the large  $N(f)$  limit of chiral perturbation theory. Phys. Lett. B. 1992;286:136-146.
20. Hyams B, et al. Phase Shift Analysis from 600-MeV to 1900-MeV. Nucl. Phys. B. 1973;64:134-162.
21. Grayer G, et al. High Statistics Study of the Reaction  $\pi^-p \rightarrow \pi^- \pi^+ n$ ; Apparatus, Method of Analysis, and General Features of Results at 17-GeV/c. Nucl. Phys. B. 1974;75:189-245.
22. Batley JR, et al. Precise tests of low energy QCD from  $K(e4)$  decay properties. Eur. Phys. J. C. 2010;70:635-657.
23. García-Martin R, et al. Precise determination of the  $f_0(600)$  and  $f_0(980)$  pole parameters from a dispersive data analysis. Phys. Rev. Lett. 1974;107:072001.
24. Gomez Nicola A, et al. Finite temperature pion scattering to one loop in chiral perturbation theory. Phys. Lett. B. 1974;550:55-64.
25. Zinn-Justin J. Quantum Field Theory and Critical phenomena. 2002.
26. Olive KA, et al. Review of Particle Physics. Chin. Phys. C. 2014;38:090001.